Band structure of an effective-mass superlattice

V. Milanović
Faculty of Electrical Engineering, Bulevar Revolucije 73, Belgrade, Yugoslavia
and High Technical Post Telegraph and Telephone School, Zdravka Čelara 16, Belgrade, Yugoslavia

Z. Ikonić
Faculty of Electrical Engineering, Bulevar Revolucije 73, Belgrade, Yugoslavia
(Received 19 October 1987)

The miniband structure of an effective-mass superlattice is analyzed within the effective-mass envelope-function approximation. The dependence of the full energy on the wave vector (longitudinal and transverse components) is derived. Expressions for finding zero energy gaps are given. Numerical results show that pronounced nonparabolicity of the energy variation with transverse wave vector, and zero energy gaps, occur in the energy region important for evaluation of macroscopic properties of this type of superlattice (10–100 meV).

Recently a new type of compositional superlattice, the effective-mass superlattice (EMSL), was proposed by Sasaki[1] where the effective mass of electrons or holes is changed periodically and the conduction- or valence-band edges are aligned. A number of candidate materials for this type of superlattice is given in Refs. 1 and 2. In the case of effective-mass variation, it is known that the effective potential on the carriers depends qualitatively on the transverse component of their wave vectors.[3] In this paper we shall discuss the EMSL band structure taking this effect into account.

We treat an EMSL composed of semiconductor layers I and II, with thicknesses d_1 and d_2 (Fig. 1). We take their conduction-band edges to be aligned (certainly for the valence band this is not necessarily so, but it is of no importance here). Within the effective-mass approximation electron motion is described by

$$-\frac{\hbar^2}{2}\frac{d}{dz}\left[\frac{1}{m(z)}\frac{d\psi}{dz}\right]+U_{\mathrm{eff}}(z)\psi=E\psi\ ,$$
$$U_{\mathrm{eff}}(z)=\frac{\hbar^2k_t^2}{2m(z)} \qquad (1)$$

where ψ is the envelope wave function, k_t the transverse wave vector, E the total electron energy, and $m(z)$ equals m_1 and m_2 in materials I and II (for simplicity we take isotropic effective mass). The effective potential $U_{\mathrm{eff}}(z)$ for $k_t=0$ is z independent and is taken as zero. For nonzero k_t, however, $U_{\mathrm{eff}}(z)$ is not constant and has a rectangular variation, as does the effective mass. Taking $m_1>m_2$, layers I become wells and layers II become barriers, as depicted in Fig. 1 by the dashed line.

Applying the conventional Bloch boundary conditions we arrive at the $E(\mathbf{k})$ dependence. For $E\geq\hbar^2k_t^2/(2m_2)$ it reads

$$-\frac{r^{1/2}(E-E_{t2})+r^{-1/2}(E-E_{t1})}{2[(E-E_{t1})(E-E_{t2})]^{1/2}}\sin(k_1d_1)\sin(k_2d_2)+\cos(k_1d_1)\cos(k_2d_2)=\cos(k_zd)\ ,$$
$$r=m_1/m_2,\quad k_{1,2}^2=\frac{2m_{1,2}(E-E_{t1,t2})}{\hbar^2},\quad E_{t1,t2}=\frac{\hbar^2k_t^2}{m_{1,2}},\quad d=d_1+d_2\ . \qquad (2)$$

For $E<\hbar^2k_t^2/(2m_2)$, $\sin(k_2d_2)$ and $\cos(k_2d_2)$ should be replaced by $i\sinh(k_2'd_2)$ and $\cosh(k_2'd_2)$, where $k_2'=ik_2$. The above energy spectrum is minibandlike with band edges determined by $\cos(k_zd)=\pm1$. Following Allen (Ref. 4) we factorize the expression (2) for $\cos(k_zd)=1$ as

$$(\lambda v\,tg v+u\,tg u)(\lambda v\,ctg v+u\,ctg u)=0\ ,$$
$$u=k_1d_1/2,\quad v=k_2d_2/2,\quad \lambda\equiv(m_1d_1)/(m_2d_2) \qquad (3)$$

and for $\cos(k_zd)=-1$ as

$$(\lambda v\,ctg v-u\,tg u)(\lambda v\,tg v-u\,ctg u)=0\ . \qquad (4)$$

The wave functions at the band edges being either even or odd, we get energies corresponding to even and odd wave functions by equating the first and the second factors of (3) and (4) to zero, respectively.

It is an interesting point here to investigate the existence of zero-energy gaps (ZEG's) in the (E,k_t^2) plane. If for some definite k_t both factors of (3) or (4) happen to be zero, the wave function has no definite parity and the energy gap vanishes [two neighboring band-edge $E(k_t^2)$ lines cross each other here].

The first ZEG condition is given by

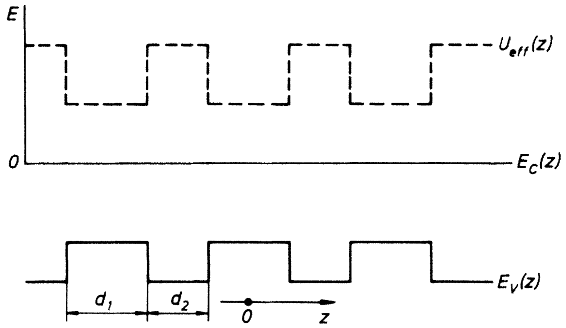

FIG. 1. Effective potential in an EMSL for $k_t = 0$ (solid lines) and $k_t > 0$ (dashed lines).

$$u = \frac{n\pi}{2} \quad \text{and} \quad v = \frac{l\pi}{2}, \quad l,n = 1,2,3, \ldots \tag{5}$$

where $l+n$ should be even for $k_z = 0$ and odd for $k_z = \pi/d$. The second ZEG condition takes the form

$$v = \frac{\pi}{2}\frac{s}{1+\lambda} \quad \text{and} \quad u = \lambda v, \quad s = 1,2,3, \ldots \tag{6}$$

where s is even for $k_z = 0$ and odd for $k_z = \pi/d$. Thus, from (5) and (6), points (E_0, k_{t0}) satisfying either of these two ZEG conditions may be found.

Furthermore, one can derive that the slopes of the band-edge $E(E_{t1})$ lines at ZEG points given by (5) are

$$\frac{dE}{dE_{t1}} = \lambda_1 = \frac{r+\Delta}{1+\Delta}, \tag{7}$$

or

$$\frac{dE}{dE_{t1}} = \lambda_2 = \frac{r + r^2\nu^2\Delta^3}{1 + r^2\nu^2\Delta^3}, \quad \Delta = \frac{d_1}{d_2} \quad \text{and} \quad \nu = \frac{l}{n} \tag{8}$$

where (7) applies for (i) $k_z = 0$, l, and n even, even wave function, (ii) $k_z = 0$, l, and n odd, odd wave function, (iii) $k_z = \pi/d$, n even, l odd, even wave function, and (iv) $k_z = \pi/d$, n odd, l even, odd wave function, while (8) holds for the rest of the cases.

At ZEG points given by (6) slopes are given by

$$\frac{dE}{dE_{t1}} = \frac{r^2+\theta}{r+\theta}, \quad \theta = \frac{\sin(2\lambda v) \mp 2\lambda v}{\sin(2v) \mp 2v} \times \begin{cases} \dfrac{\sin^2 v}{\sin^2(\lambda v)} & \text{for } k_z = 0,\ s \text{ even, even wave function and} \\ & k_2 = \pi/d,\ \ s \text{ odd, odd wave function} \\ \dfrac{\cos^2 v}{\cos^2(\lambda v)} & \text{otherwise}\ . \end{cases} \tag{9}$$

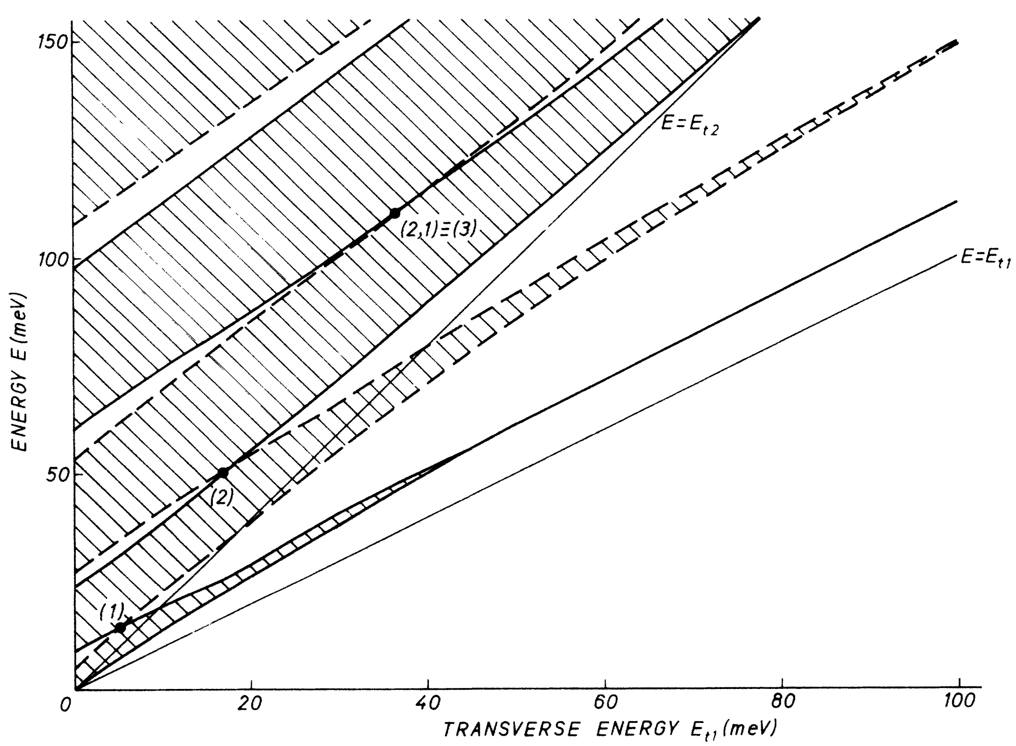

FIG. 2. Energy-band diagram for an EMSL with $d_1 = d_2 = 100$ Å and $m_1 = 2m_2 = 0.2m_0$. The crosshatched areas denote the allowed bands. The solid (dashed) band-edge lines correspond to even (odd) wave functions. Points of line intersection are labeled with (l,n) where l and n are integers in Eq. (5), or with (s) the integer in Eq. (6). Note that points (2,1) and (3) coincide.

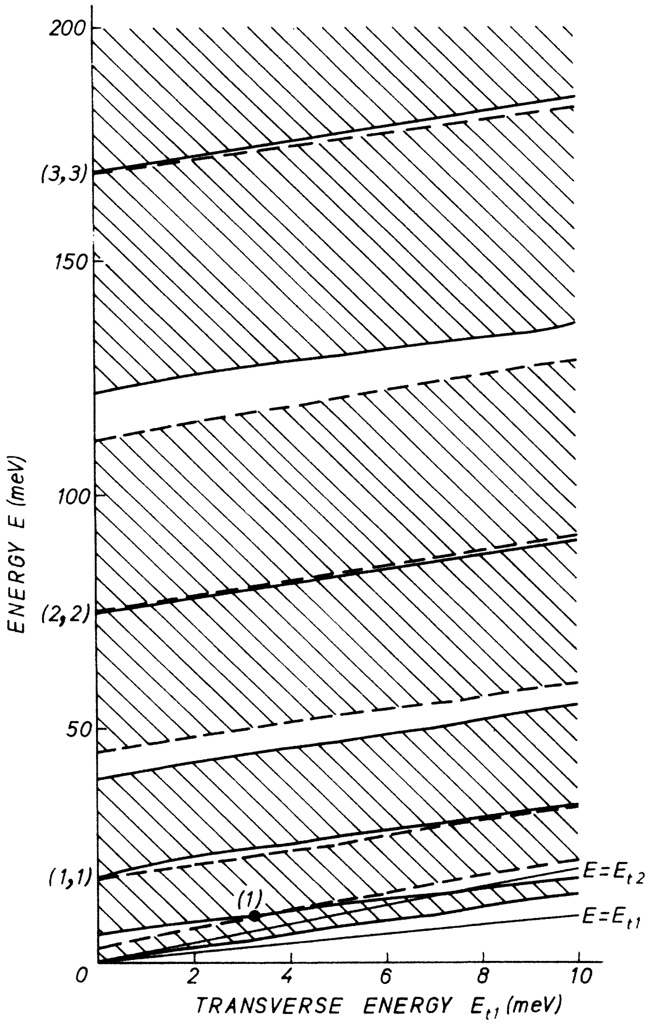

FIG. 3. Energy-band diagram for an EMSL with $d_1=100$ Å, $m_1=2m_2=0.2m_0$, and $m_1d_1^2=m_2d_2^2$, for small k_t values. Pairs of neighboring minibands touch at $k_t=k_z=0$.

Finally, we shall briefly analyze a special case, $m_1d_1^2=m_2d_2^2$, mentioned by Sasaki,[1,2] which enables explicit solution for band edges at $k_t=0$. We find that for $k_z=0$ all solutions of Eq. (2) fulfill the ZEG's condition, while for $k_z=\pi/d$ band gaps ΔE_{gp} exist and are given by

$$\Delta E_{gp}=E_0\pi(p-\tfrac{1}{2})(2\arctan R-\pi/2)\ ,$$

$$R\equiv\left[\frac{m_1}{m_2}\right]^{1/4}=\left[\frac{d_2}{d_1}\right]^{1/2},\quad E_0=\frac{\hbar^2\pi^2}{2m_1d_1^2}\ , \tag{10}$$

where $p=1,2,3,\ldots$ for subsequent gaps.

The full width of two touching (at $k_z=0$) allowed bands ΔE_{ap} are

$$\Delta E_{ap}=\begin{cases}E_0(\arctan R)^2, & p=1\\ E_0(p-1)(\pi-2\arctan R), & p=2,3,4,\ldots\ .\end{cases} \tag{11}$$

According to Refs. 1, 2, and 5 the effective mass ratio of 1.4 at most may be achieved in an unstrained EMSL, while higher values may be obtained by introducing the strained-layer EMSL. For numerical illustration, in Fig. 2 we give the $E(E_{t1})$ band diagram for a hypothetical, but roughly realistic EMSL, with $m_1=2m_2=0.2m_0$ (m_0 is the free-electron mass), with layers each 100 Å thick. What can immediately be seen from Fig. 2 is that the ZEG's in the EMSL occur for much lower energies E and E_{t1} than is the case in conventional (e.g., GaAs-$\mathrm{Al}_x\mathrm{Ga}_{1-x}\mathrm{As}$) superlattices, where ZEG points may be calculated to be in the eV range[3] and are therefore hardly of any significance for most of macroscopic properties. In the EMSL ZEG points fall in a thermically populated energy range, and thus do influence the EMSL properties, e.g., carrier concentration, absorption, etc. Excluding the band-edge discontinuities, $E(k_t^2)$ dependence in an EMSL is pronouncedly nonlinear (Fig. 2).

Furthermore, a very interesting point is the inversion of parity of band-edge wave functions when crossing ZEG points; e.g., for small k_t the top of the first miniband possesses the odd wave function, and not the even one, as does its bottom. Only after crossing the ZEG's point does the wave-function parity at both bottom and top become the same (even for odd minibands and vice versa, for high enough transverse wave vector k_t). This fact may be important when evaluating optical transition matrix elements because their values may turn from finite ones to zero for small change of k_t.

We also note that no ZEG's may appear for energies $E<E_{t2}$. With increasing k_t the effective barriers (layers II) get higher, which makes the allowed bands progressively narrower and eventually nearly discrete (this happens at realistic values of E_{t1}, a couple of kT at $T=300$ K).

In Fig. 3 the band diagram of the EMSL with $m_1d_1^2=m_2d_2^2$ for small $E_{t1}\le 10$ meV is given. As discussed above, ZEG points occur at $k_z=k_t=0$ and two allowed bands touch here, but with increasing k_t gaps appear. The two band-edge lines emerge from these ZEG points with slopes given by (8).

In conclusion, results of this work may be useful for more exact evaluation of the EMSL macroscopic properties, as well as for analyzing, e.g., the performance of possible negative resistance devices based on it. It was noted in Ref. 5 that the switches based on resonant electron tunneling in the EMSL should have an order of magnitude lower threshold voltages and 2 orders greater current density than those with conventional superlattices. The pronounced nonparabolicity of $E(k_t^2)$ in the EMSL may also find some applications, e.g., in nonlinear optics.

[1]A. Sasaki, Phys. Rev. B **30**, 7016 (1984).
[2]A. Sasaki, Surf. Sci. **174**, 624 (1986).
[3]V. Milanović and D. Tjapkin, Phys. Status Solidi B **110**, 687 (1982); V. Milanović, D. Tjapkin, and Z. Ikonić, Phys. Rev. B **34**, 7404 (1986).
[4]G. Allen, Phys. Rev. **91**, 531 (1953).
[5]A. Aishima and Y. Fukushima, J. Appl. Phys. **61**, 249 (1987).